Supplementary Material for "Reversible signal transmission in an active mechanical metamaterial"

Alexander P Browning[1,2], Francis G Woodhouse[3], Matthew J Simpson[1]

[1] Mathematical Sciences, Queensland University of Technology, Brisbane, Australia
[2] ARC Centre of Excellence for Mathematical and Statistical Frontiers, QUT, Australia
[3] Mathematical Institute, University of Oxford, Oxford, UK

Contents

THE ROYAL SOCIETY
PUBLISHING

S1. Numerical solution of the continuous model

In this section, we explain the numerical scheme used to solve the continuous model in the main paper. The non-dimensional continuous model is given by

$$\begin{aligned} 0 &= \frac{\partial^2 \hat{u}}{\partial \hat{t}^2} - \frac{\partial^2 \hat{u}}{\partial \hat{x}^2} + \frac{\partial \hat{u}}{\partial \hat{t}} + \nu(\hat{u}^2 - 1)\left(\frac{\hat{u}}{\eta} - \hat{a}\right), \\ 0 &= \frac{\partial \hat{a}}{\partial \hat{t}} - \kappa\left(\frac{\hat{u}}{\eta} - \hat{a}\right), \end{aligned} \tag{S1.1}$$

where $\hat{x} \in (0, L)$, with no-flux boundary conditions on $\hat{x} \in \{0, \hat{L}\}$, and initial conditions given by

$$\begin{aligned} \hat{u}(\hat{x}, 0) &= \begin{cases} 1, & 0 \le \hat{x} < Q, \\ -1, & Q \le \hat{x} \le \hat{L}, \end{cases} \\ \hat{a}(\hat{x}, 0) &= \begin{cases} 1/\eta, & 0 \le \hat{x} < Q, \\ -1/\eta, & Q \le \hat{x} \le \hat{L}. \end{cases} \end{aligned} \tag{S1.2}$$

To solve the system given by equation (S1.1), we employ a finite difference technique. We first introduce

$$\hat{w} = \frac{\partial \hat{u}}{\partial \hat{t}}, \tag{S1.3}$$

so that the system in equation (S1.1) can be written as the first order system of partial differential equations (PDEs),

$$\begin{aligned} \frac{\partial \hat{u}}{\partial t} &= \hat{w}, \\ \frac{\partial \hat{w}}{\partial t} &= \frac{\partial^2 \hat{u}}{\partial \hat{x}^2} - \hat{w} - \nu(\hat{u}^2 - 1)(\hat{u} - \hat{a}), \\ \frac{\partial \hat{a}}{\partial \hat{t}} &= \kappa\left(\frac{\hat{u}}{\eta} - \hat{a}\right). \end{aligned} \tag{S1.4}$$

Initially, the system is at rest, so that

$$\hat{w}(\hat{x}, 0) = 0. \tag{S1.5}$$

Next, we divide the domain, $\hat{x} \in [0, \hat{L}]$ into S equally spaced subintervals, each of width $\delta\hat{x} = \hat{L}/S$. We index the boundary of each subinterval with $n \in \{0, 1, ..., S\}$, such that $\hat{u}_n(t) \approx \hat{u}(n\delta\hat{x}, \hat{t})$. Doing this, we obtain the following system of first order, non-linear, ordinary differential equations,

$$\begin{aligned} \frac{\mathrm{d}\hat{u}_n}{\mathrm{d}t} &= \hat{w}_n, \ \forall n, \\ \frac{\mathrm{d}\hat{w}_0}{\mathrm{d}t} &= \frac{\hat{u}_1 - \hat{u}_0}{\Delta x^2} - \hat{w}_1 - \nu(\hat{u}_0^2 - 1)(\hat{u}_0 - \hat{a}_0), \\ \frac{\mathrm{d}\hat{w}_n}{\mathrm{d}t} &= \frac{\hat{u}_{n+1} - 2\hat{u}_n + \hat{u}_{n-1}}{\Delta x^2} - \hat{w}_n - \nu(\hat{u}_n^2 - 1)(\hat{u}_n - \hat{a}_n), \ 1 \le n \le S-1, \\ \frac{\mathrm{d}\hat{w}_S}{\mathrm{d}t} &= \frac{\hat{u}_S - \hat{u}_{S-1}}{\Delta x^2} - \hat{w}_S - \nu(\hat{u}_S^2 - 1)(\hat{u}_S - \hat{a}_S), \\ \frac{\mathrm{d}a_i}{\mathrm{d}t} &= \kappa\left(\frac{\hat{u}_n}{\eta} - \hat{a}_n\right) \ \forall n. \end{aligned} \tag{S1.6}$$

Next, we let $\mathbf{X}(t) = \langle \hat{u}_0, ..., \hat{u}_S, \hat{w}_0, ..., \hat{w}_S, \hat{a}_0, ..., \hat{a}_S \rangle$ such that equation (S1.6) can be written as $\mathbf{X}' = \mathbf{f}(\mathbf{X})$. We can then integrate equation (S1.6) using a second order trapezoidal rule,

$$\frac{\mathbf{X}(t + \Delta t) - \mathbf{X}(t)}{\Delta t} \approx \frac{1}{2}\Big(\mathbf{f}[\mathbf{X}(t + \Delta t)] + \mathbf{f}[\mathbf{X}(t)]\Big). \tag{S1.7}$$

We solve equation (S1.7) using Picard iteration [1], where $\mathbf{X}(t)$, which is always known, is taken to be the initial guess at each timestep. The initial conditions are chosen according to equations (S1.2) and (S1.5).

Unless specified otherwise, results in the main paper are produced using a discretisation where $\delta t = 0.01$ and $S = 10000$.

S2. Signal initiation

In the main text, we focus on the materials ability to transmit signals that are initiated at the left boundary. In addition to this, results shown in the main text allow sufficient time between signal reception at the right boundary and retransmission. In figure S1 we demonstrate how a second signal initiated from the right boundary at $t_2 = 344$ is unable to propagate, whereas a second signal initiated from the right boundary at $t_2 = 345$ is able. In figure S2 we demonstrate that a second signal initiated from the left boundary at $t_2 = 80$ is unable to propagate, whereas those initiated at $t_2 = 90$ and $t_2 = 100$ are able, albeit with an initially slower transmission speed. Finally, in figure S3 we show how two signals initiated simultaneously from both the left and right boundaries collide.

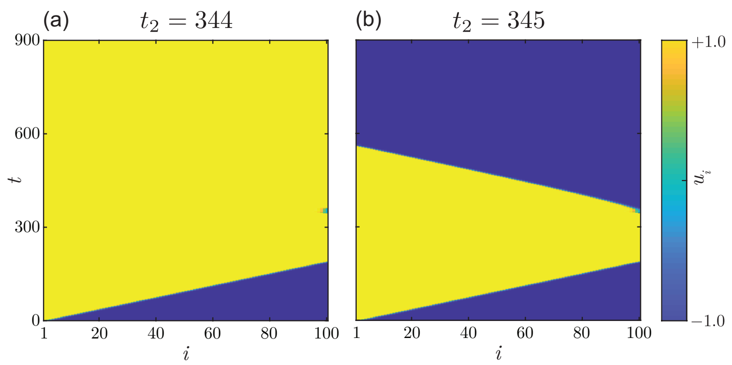

Figure S1. Signal propagation through the material described by the discrete model showing $u_i(t)$, the displacement, where i is the mass index. The first signal was initiated by moving the first element from a displacement of $-\delta$ to δ at $t = 0$, and was retransmitted by moving the last element from a displacement of δ to $-\delta$ at $t = t_2$. In (a) the second signal was not able to propagate for this value of ϵ, in (b) the signal is able to propagate. Parameters used are $m = 1$ g, $k = 1$ g m/s^2, $\gamma = 1$ g/s, $\Delta = 0.002$ m, $\delta = 1$ m, $\epsilon = 0.01$ /s, $\eta = 2$, $v = 1$ g/(m^{2}s^2) and $N = 101$ masses.

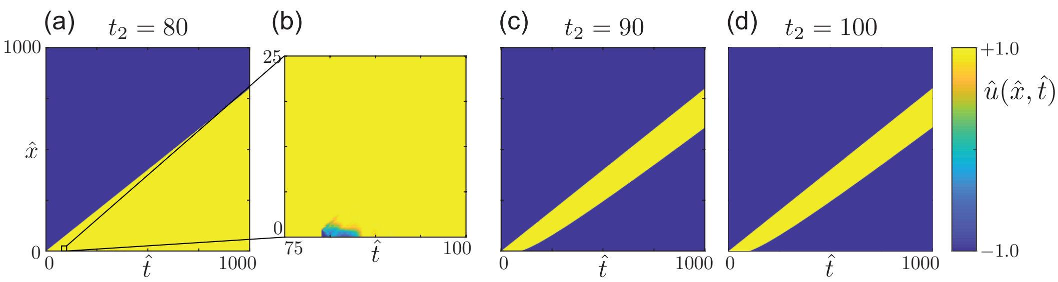

Figure S2. The solution to the continuous model showing $\hat{u}(\hat{x}, \hat{t})$. The first signal is initiated by setting $\hat{u}(\hat{x}, \hat{t}) = 1$ for $\hat{x} < 1$ at $t = 0$. The second signal was initiated by setting $\hat{u}(\hat{x}, \hat{t}) = -1$ for $\hat{x} < 1$ at $t = t_2$. In (a) the second signal is not able to propagate (signal initiation is shown in the inset (b)). In (c) and (d), the second signal is able to propagate.

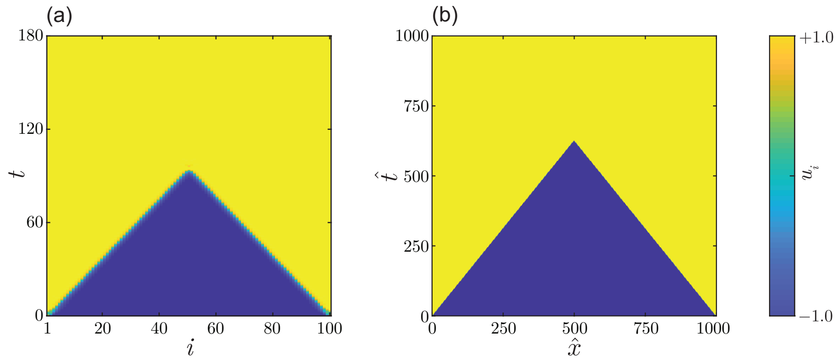

Figure S3. (a) The solution to the discrete model showing showing $u_i(t)$, the displacement, where i is the mass index. A signal is initiated simultaneously at each end of the domain by moving the first and last element to $u_i = 1$ at $t = 0$. (b) The solution to the continuous model showing the displacement field, $\hat{u}(\hat{x}, \hat{t})$. A signal is initiated simultaneously at each end of the domain by setting $\hat{u}(\hat{x}, \hat{t}) = -1$ for $\hat{x} \leq 1$ and $\hat{x} \geq 499$ at $t = 0$. The parameters used in the discrete model are $m = 1$ g, $k = 1$ g m/s^2, $\gamma = 1$ g/s, $\varDelta = 0.002$ m, $\delta = 1$ m, $\epsilon = 0.01$ /s, $\eta = 2$, $v = 1$ g/(m^{2}s^2) and $N = 101$ masses. The parameters used in the continuous model are $\nu = 4$, $\eta = 2$ and $\kappa = 0.01$.

S3. Wavespeed approximation technique

In this section, we detail the technique we use to approximate the wavespeed, c, from the solution of the continuous model. The technique used to solve the continuous model numerically is described in section S1. The numerical parameters used to solve the continuous model: for the purpose of estimating the wavespeed in table 1 in the main paper, are shown in table S1; and, for the purpose of estimating the wavespeed in figure 7 in the main paper, are shown in table S2.

We first convert space-time data to wave-location time series data by defining the location of the front, $x_0(t)$, where

$$\hat{x}_0(t) = \hat{x} \,:\, \hat{u}(\hat{x}, \hat{t}) = 0. \tag{S3.1}$$

As our data is typically discrete, we find $x_0(t)$ using a linear interpolation. We now have discrete data for $\hat{x}_0(t)$ where $0 \leq \hat{t} \leq \hat{t}_{\text{max}}$. An example of this data is shown in figure S4a.

Next, we determine a section of the wavefront curve that is at "late time" and sufficiently far from the right boundary. In this study, we found an appropriate region, to be automatically determined as

$$\hat{t} \in (\hat{t}_{\text{lower}}, \hat{t}_{\text{upper}}) = (0.8\hat{t}_{\text{max}}, 0.9\hat{t}_{\text{max}}). \tag{S3.2}$$

This process gives us (approximately) linear data of the form $\{t^{(i)}, x_0^{(i)}\}$, where the slope is the estimate of the wavespeed, c. An example of this (approximately) linear data is shown in figure S4b.

To approximate c, we linearly interpolate the data $\{t^{(i)}, x_0^{(i)}\}$, and choose c to be the gradient of the regression line.

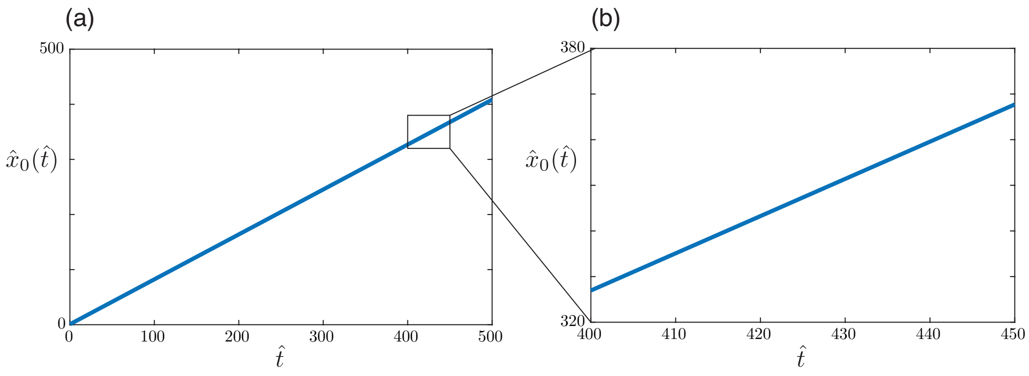

Figure S4. Example wave front time series data, produced using a solution to the continuous model for $\nu = 4$, $\eta = 2$ and $\kappa = 0$. Numerical parameters are detailed in table S1. (a) Shows the front data for $\hat{t} \in [0, \hat{t}_{\max}]$. (b) Shows the inset of (a) where $\hat{t} \in (\hat{t}_{\text{lower}}, \hat{t}_{\text{upper}})$, which corresponds to data from which the wavespeed is approximated from.

η	ν	$\hat{t}_{\max}$	$\hat{x}_{\max}$	$\delta\hat{t}$	S
1.5	1	500	500	0.01	10000
1.5	2	500	500	0.01	10000
1.5	4	500	500	0.01	10000
2	1	500	500	0.01	10000
2	2	500	500	0.01	10000
2	4	500	500	0.01	10000
3	1	500	500	0.01	10000
3	2	500	500	0.01	10000
3	4	500	500	0.01	10000
4	1	500	2000	0.01	20000
4	2	500	2000	0.01	20000
4	4	500	2000	0.01	20000

Table S1. Numerical parameters used to solve the continuous model when estimating the wavespeed for $\kappa \ll 1$ in table S3 of this supporting material document.

η	ν	$\hat{t}_{\max}$	$\hat{x}_{\max}$	$\delta\hat{t}$	S
1.5	1	500	10000	0.01	10000
1.5	2	500	1000	0.01	10000
1.5	4	500	1000	0.01	10000
2	1	500	10000	0.01	10000
2	2	500	1000	0.01	10000
2	4	500	1000	0.01	10000
3	1	500	10000	0.01	10000
3	2	500	1000	0.01	10000
3	4	500	1000	0.01	10000
4	1	500	10000	0.01	20000
4	2	500	10000	0.01	20000
4	4	500	10000	0.01	20000

Table S2. Numerical parameters used to solve the continuous model when estimating the wavespeed for $\kappa > 0$ in figure 7 in the main document.

S4. Perturbation solution

In this section, we present our method for finding a singular perturbation expansion to the travelling wave model, given by the system

$$0 = \frac{\mathrm{d}^2 f}{\mathrm{d}z^2} + \frac{c}{1-c^2}\frac{\mathrm{d}f}{\mathrm{d}z} - \frac{\nu}{1-c^2}(f^2-1)(f-h), \quad f(\pm\infty) = \mp 1, \tag{S4.1}$$

$$0 = \frac{\mathrm{d}h}{\mathrm{d}z} + \frac{\kappa}{c}\left(\frac{f}{\eta} - h\right), \quad h(\infty) = -\frac{1}{\eta}, \tag{S4.2}$$

We pose a perturbation expansion for the wavespeed,

$$c = c_0 + c_1\kappa + \mathcal{O}(\kappa^2), \tag{S4.3}$$

where c_0 is known. We take time to note that, for this expansion, we also have

$$\frac{1}{c} = \frac{1}{c_0} - \frac{c_1}{c_0^2}\kappa + \mathcal{O}(\kappa^2).$$

$$\frac{c}{1-c^2} = \frac{c_0}{1-c_0^2} + \left(\frac{c_1}{1-c_0^2} + \frac{2c_0^2 c_1}{(1-c_0^2)^2}\right)\kappa + \mathcal{O}(\kappa^2),$$

$$\frac{\nu}{1-c^2} = \nu\left(\frac{1}{1-c_0^2} + \frac{2c_0 c_1}{(1-c_0^2)^2}\kappa + \mathcal{O}(\kappa^2)\right).$$

We now proceed to find perturbation solutions in the inner and outer regions. We denote solutions in the inner region $z \sim \mathcal{O}(\mu_0^{-1})$ using lowercase variables, $f(z)$ and $h(z)$. We denote solutions in the outer region $Z = \kappa z \sim \mathcal{O}(\kappa^{-1})$ using uppercase variables, $F^{(L)}(Z)$, $F^{(R)}(Z)$, $H^{(L)}(Z)$ and $H^{(R)}(Z)$, where a superscript, (L) and (R), denotes solutions in left, $Z < 0$ and right, $Z > 0$ regions of the outer region, respectively.

Outer Region

Substituting $Z = \kappa z$ into equations (S4.1) and (S4.2) leads to a system described by

$$\begin{aligned} 0 &= \kappa^2\frac{\mathrm{d}^2 F}{\mathrm{d}Z^2} + \frac{c\kappa}{1-c^2}\frac{\mathrm{d}F}{\mathrm{d}Z} - \frac{\nu}{1-c^2}(F^2-1)(F-H), \\ 0 &= \frac{\mathrm{d}H}{\mathrm{d}Z} + \frac{1}{c}\left(\frac{F}{\eta} - H\right), \end{aligned} \tag{S4.4}$$

The left and right solutions in the outer region will match the corresponding left and right boundary conditions from equations (S4.1) and (S4.2), such that

$$F^{(L)}(-\infty) = 1, \qquad H^{(L)}(-\infty) = \frac{1}{\eta}, \tag{S4.5}$$

$$F^{(R)}(\infty) = -1, \qquad H^{(R)}(\infty) = -\frac{1}{\eta}. \tag{S4.6}$$

Provided $\kappa \ll \mu_0$, for $Z \sim \mathcal{O}(1)$ the solution to the system for $\kappa = 0$ is given by

$$f\left(\frac{Z}{\kappa}\right) = \tanh\left(\frac{\mu_0}{\kappa}Z\right) \sim -\mathrm{sign}(Z),$$

since $\mu_0/\kappa \ll 1$. It is then trivial to see that the expansion for $F(Z)$ contains only the leading order term, so that

$$F(Z) = -\mathrm{sign}(Z) \Rightarrow \begin{array}{ll} F^{(L)}(Z) = 1, & Z < 0, \\ F^{(R)}(Z) = -1, & Z > 0. \end{array} \tag{S4.7}$$

Therefore, the solution for $H(Z)$ where $Z > 0$, $H^{(R)}(Z)$, is given by

$$H^{(R)}(Z) = -\frac{1}{\eta}. \tag{S4.8}$$

To find the solution for $H(Z)$ where $Z<0$, $H^{(L)}(Z)$, we pose a perturbation solution of the form

$$H^{(L)}(Z)=H_0+H_1\kappa+\mathcal{O}(\kappa^2). \tag{S4.9}$$

Substituting this perturbation expansion into equation (S4.4) gives

$$0=H_0'+\frac{1}{c_0}\left(\frac{1}{\eta}-H_0\right)+\left[H_1'-\frac{1}{c_0}H_1+\frac{c_1}{c_0^2}\left(\frac{1}{\eta}-H_0\right)\right]\kappa+\mathcal{O}(\kappa^2), \tag{S4.10}$$

where the boundary conditions are given by

$$\lim_{Z\to-\infty}=\begin{cases}-\dfrac{1}{\eta}, & i=0,\\ 0, & i>1.\end{cases} \tag{S4.11}$$

The $\mathcal{O}(1)$ term in equation (S4.10) gives the separable ordinary differential equation

$$0=H_0'+\frac{1}{c_0}\left(\frac{1}{\eta}-H_0\right),\ Z<0,\ \lim_{Z\to-\infty}H_0(Z)=\frac{1}{\eta}, \tag{S4.12}$$

which has the solution

$$H_0(Z)=\alpha_1\exp\left(\frac{Z}{c_0}\right)+\frac{1}{\eta},$$

where α_1 is to be determined by matching solutions in the inner and outer regions to $\mathcal{O}(1)$.

The $\mathcal{O}(\kappa)$ term in equation (S4.10) gives the ordinary differential equation

$$0=H_1'-\frac{1}{c_0}H_1+\frac{c_1}{c_0^2}\alpha_1\exp\left(\frac{Z}{c_0}\right),\ Z<0,\ \lim_{Z\to-\infty}H_1(Z)=0, \tag{S4.13}$$

which has the solution

$$H_1(Z)=\left(\alpha_2-\frac{c_1}{c_0^2}\alpha_1 Z\right)\exp\left(\frac{Z}{c_0}\right), \tag{S4.14}$$

where α_2 is to be determined by matching solutions in the inner and outer regions to $\mathcal{O}(\kappa)$.

Inner Region

In the inner region, we pose a perturbation solution of the form

$$f(z)=f_0(z)+f_1(z)\kappa+\mathcal{O}(\kappa^2), \tag{S4.15}$$

$$h(z)=h_0(z)+h_1(z)\kappa+\mathcal{O}(\kappa^2), \tag{S4.16}$$

where f_0 and h_0 are the solutions for $\kappa=0$,

$$f_0(z)=-\tanh(\mu_0 z), \tag{S4.17}$$

$$h_0(z)=-\frac{1}{\eta}. \tag{S4.18}$$

Substituting equations (S4.15) and (S4.16) into equations (S4.1) and (S4.2) gives

$$\begin{aligned}0=&\frac{\mathrm{d}^2 f_0}{\mathrm{d}z^2}+\frac{1}{c_0}\frac{\mathrm{d}f_0}{\mathrm{d}z}-\frac{\nu}{1-c_0^2}(f_0^2-1)(f_0-h_0)\\&+\left\{\frac{\mathrm{d}^2 f_1}{\mathrm{d}z^2}+\frac{1}{c_0}\frac{\mathrm{d}f_1}{\mathrm{d}z}-\frac{\nu}{1-c_0^2}\Big(2f_0(f_0-h_0)+(f_0^2-1)\Big)f_1\right.\\&+\left(\frac{c_1}{1-c_0^2}+\frac{2c_0^2c_1}{(1-c_0^2)^2}\right)\frac{\mathrm{d}f_0}{\mathrm{d}z}-\frac{2\nu c_0c_1}{(1-c_0^2)^2}(f_0^2-1)(f_0-h_0)\\&\left.+\frac{\nu}{1-c_0^2}(f_0^2-1)h_1\right\}\kappa+\mathcal{O}(\kappa^2),\end{aligned} \tag{S4.19}$$

$$0=\frac{\mathrm{d}h_0}{\mathrm{d}z}+\left\{\frac{\mathrm{d}h_1}{\mathrm{d}z}+\frac{1}{c_0}\left(\frac{f_0}{\eta}-h_0\right)\right\}\kappa+\mathcal{O}(\kappa^2). \tag{S4.20}$$

The $\mathcal{O}(\kappa^1)$ term in equation (S4.20) is directly integrable. Consider

$$0 = \frac{\mathrm{d}h_1}{\mathrm{d}z} + \frac{1}{c_0}\left(\frac{f_0}{\eta} - h_0\right), \tag{S4.21}$$

which has solution

$$h_1(z) = \frac{1}{c_0\mu_0\eta}\Big(\log(\cosh(\mu_0 z)) - \mu_0 z + \alpha_3\Big), \tag{S4.22}$$

where α_3 is to be determined by matching solutions in the inner and outer regions to $\mathcal{O}(\kappa)$.

To solve for $f_1(z)$, we consider that the $\mathcal{O}(\kappa^1)$ term in equation (S4.19) can be written as

$$0 = \frac{\mathrm{d}^2 f_1}{\mathrm{d}z^2} + p(z)\frac{\mathrm{d}f_1}{\mathrm{d}z} + q(z) f_1 + c_1 r(z) + s(z), \quad \lim_{z\to\pm\infty} f_1(z) = 0, \tag{S4.23}$$

where c_1 is a yet undetermined correction term to the wave-speed, and

$$\begin{aligned}
p(z) &= \frac{1}{c_0},\\
q(z) &= -\frac{\nu}{1-c_0^2}\left(3\tanh^2(\mu_0 z) - \frac{2}{\eta}\tanh(\mu_0 z) - 1\right),\\
r(z) &= -\frac{\operatorname{sech}^2(\mu_0 z)}{1-c_0^2}\left[\mu_0\left(1 + \frac{2c_0^2}{1-c_0^2}\right) + \frac{2c_0\nu}{1-c_0^2}\left(\tanh(\mu_0 z) - \frac{1}{\eta}\right)\right],\\
s(z) &= -\frac{\nu\operatorname{sech}^2(\mu_0 z)}{(1-c_0^2)c_0\mu_0 Okap\eta}\left(\log(\cosh(\mu_0 z)) - \mu_0 z + \log(2)\right).
\end{aligned} \tag{S4.24}$$

The boundary conditions are chosen so that $f_1(z)$ is able to match the correction term in the outer solution, $F_1(Z) \equiv 0$. We describe the numerical technique we use to solve this boundary value problem in section S6 of this supporting material document.

Matching

Here, we apply van Dyke's matching rule [2] to determine the integration constants that have appeared in each solution.

First, we match the fast solution to the slow right solution to $\mathcal{O}(\kappa)$,

$$\begin{aligned}
\lim_{\kappa\to 0} H^{(R)}(\kappa z) &= \lim_{\kappa\to\infty}\left[h_0\left(\frac{Z}{\kappa}\right) + h_1\left(\frac{Z}{\kappa}\right)\kappa\right],\\
-\frac{1}{\eta} &= -\frac{1}{\eta} + \lim_{\kappa\to\infty}\frac{1}{c_0\mu\eta}\left(\log\left(\cosh\left(\frac{\mu}{\kappa}Z\right)\right) - \frac{\mu}{\kappa}Z + \alpha_3\right),\\
&\Rightarrow \alpha_3 = \log(2).
\end{aligned}$$

Next, we match the fast solution to the slow left solution to $\mathcal{O}(1)$,

$$\begin{aligned}
\lim_{\kappa\to 0} H_0(\kappa z) &= \lim_{\kappa\to\infty} h_0\left(\frac{Z}{\kappa}\right),\\
\lim_{\kappa\to 0}\left(\alpha_1\exp\left(\frac{\bar{c}_0\kappa\zeta}{k}\right) + \frac{1}{\eta}\right) &= \lim_{\kappa\to\infty} -\frac{1}{\eta},\\
&\Rightarrow \alpha_1 = -\frac{2}{\eta},
\end{aligned}$$

and to $\mathcal{O}(\kappa^1)$,

$$\begin{aligned}
\lim_{\kappa\to 0} H_1(\kappa z)\kappa &= \lim_{\kappa\to\infty} h_1\left(\frac{Z}{\kappa}\right)\kappa,\\
\lim_{\kappa\to 0}\left(\alpha_2 - \frac{2c_1}{\eta c_0^2}\kappa z\right)\exp\left(\frac{z}{\kappa c_0}\right)\kappa &= \lim_{\kappa\to\infty}\frac{1}{c_0\mu\eta}\left(\log\left(\cosh\left(\frac{\mu}{\kappa}Z\right)\right) - \frac{\mu}{\kappa}Z + \log(2)\right)\kappa,\\
&\Rightarrow \alpha_2 = 0.
\end{aligned}$$

In summary, we have that

$$
\begin{aligned}
F(Z) &= -\mathrm{sign}(Z),\\
f(z) &= -\tanh(\mu_0 z) + f_1(z)\kappa + \mathcal{O}(\kappa^2),\\
H^{(L)}(Z) &= \frac{1}{\eta} - \frac{2}{\eta}\exp\left(\frac{Z}{c_0}\right) - \frac{2c_1}{\eta c_0^2} Z \exp\left(\frac{Z}{c_0}\right)\kappa + \mathcal{O}(\kappa^2),\\
H^{(R)}(Z) &= -\frac{1}{\eta},\\
h(z) &= -\frac{1}{\eta} + \frac{1}{c_0\mu_0\eta}\Big(\log(\cosh(\mu_0 z)) - \mu_0 z + \log(2)\Big)\kappa + \mathcal{O}(\kappa^2).
\end{aligned}
$$

S5. Numerical solution of the boundary value problem

In section S4 of this supporting material document, we find that $f_1(z)$ and c_1 are described by the boundary value problem

$$
0 = \frac{\mathrm{d}^2 f_1}{\mathrm{d}z^2} + p(z)\frac{\mathrm{d}f_1}{\mathrm{d}z} + q(z) f_1 + c_1 r(z) + s(z), \quad \lim_{z\to\pm\infty} f_1(z) = 0, \tag{S5.1}
$$

where c_1 is a yet undetermined correction term to the wavespeed, and

$$
\begin{aligned}
p(z) &= \frac{1}{c_0},\\
q(z) &= -\frac{\nu}{1-c_0^2}\left(3\tanh^2(\mu_0 z) - \frac{2}{\eta}\tanh(\mu_0 z) - 1\right),\\
r(z) &= -\frac{\mathrm{sech}^2(\mu_0 z)}{1-c_0^2}\left[\mu_0\left(1 + \frac{2c_0^2}{1-c_0^2}\right) + \frac{2c_0\nu}{1-c_0^2}\left(\tanh(\mu_0 z) - \frac{1}{\eta}\right)\right],\\
s(z) &= -\frac{\nu\,\mathrm{sech}^2(\mu_0 z)}{(1-c_0^2)c_0\mu_0\eta}\left(\log(\cosh(\mu_0 z)) - \mu_0 z + \log(2)\right).
\end{aligned} \tag{S5.2}
$$

We approximate the solution to the infinite-domain boundary value problem given by equation (S5.1) as the solution to the finite domain problem,

$$
0 = \frac{\mathrm{d}^2 Y}{\mathrm{d}z^2} + p(z)\frac{\mathrm{d}Y}{\mathrm{d}z} + q(z)Y + c_1 r(z) + s(z), \; Y(\pm L) = 0, \tag{S5.3}
$$

where $f_1(z) = \lim_{L\to\infty} Y(z)$. We find that $L = 10$ is sufficient to obtain accurate estimates of $f_1(z)$ and c_1.

Next, we divide the domain $z \in [-L, L]$ into S equally space subintervals, each of with δz. We index the boundary of each subinterval with $n \in \{0, 1, ..., S\}$, such that $Y_n(z) \approx Y(n\delta z)$. Doing this we obtain the following system of linear equations in terms of the unknowns $Y_1, ...Y_{S-1}, c_1$,

$$
\begin{aligned}
-s_n = \left(\frac{1}{\delta z^2} - \frac{p_n}{2\delta z}\right) Y_{n-1} + \left(-\frac{2}{\delta z^2} + q_n\right) Y_n + \left(\frac{1}{\delta z^2} + \frac{p_n}{2\delta z}\right) Y_{n+1} + r_n c_1,&\\
1 \le n \le S-1,&
\end{aligned} \tag{S5.4}
$$

where $Y_0 = Y_S = 0$ enforces the boundary conditions, $s_n = s(n\delta z)$, and similar for $p(z)$, $q(z)$ and $r(z)$.

Denoting the unknowns $\mathbf{X} = [Y_1, ..., Y_{S-1}, c_1]^T \in \mathbb{R}^S$, we may write the system as the underdetermined matrix system

$$
\mathbf{AX} = \mathbf{B}, \tag{S5.5}
$$

where $\mathbf{B} = [s_2, ..., s_S]^T \in \mathbb{R}^S$ and $\mathbf{A} \in \mathbb{R}^{S\times(S-1)}$. We obtain a solution $\mathbf{X}$ from the underdetermined system using the Moore-Penrose pseudoinverse [3,4] with the `pinv` command in MATLAB [4], which gives the solution with the smallest norm of all possible solutions [3,4]. We find that the component of the normalised null-space relating to the free parameter, c_1, is $\mathcal{O}(10^{-5})$, so solutions to the system of equations that have $Y(Z)$ small have similar values of the free parameter, c_1. Because of this, we find that the solution obtained from the pseudoinverse matches numerical results, obtained from the solution to the continuous model, to two significant figures, providing confidence in the approximate solution to the travelling wave obtained from the continuous model.

S6. Comparison of wavespeed calculations

η	ν	c_0		c_1		
		PDE	**Eq (3.5)**	**PDE**	**BVP**	**Eq (3.26)**
1.5	1	0.69	0.69	−0.26	−0.26	−0.30
1.5	2	0.80	0.80	−0.10	−0.10	−0.12
1.5	4	0.88	0.88	−0.03	−0.03	−0.04
2	1	0.58	0.58	−0.43	−0.43	−0.48
2	2	0.71	0.71	−0.20	−0.20	−0.22
2	4	0.82	0.82	−0.07	−0.08	−0.09
3	1	0.43	0.43	−0.67	−0.67	−0.73
3	2	0.55	0.55	−0.37	−0.37	−0.40
3	4	0.69	0.69	−0.17	−0.17	−0.19
4	1	0.33	0.33	−0.81	−0.81	−0.86
4	2	0.45	0.45	−0.49	−0.49	−0.52
4	4	0.58	0.58	−0.26	−0.27	−0.28

Table S3. Comparison of calculations of the wavespeed, c_0, and the first correction term in a perturbation solution in κ, about $\kappa = 0$, c_1, shown to two significant figures. Approximations to c_1 using the PDE are performed by fitting a fifth-order polynomial through estimates of c obtained for $\kappa \in \{0, 0.01, ..., 0.05\}$. The numerical scheme, including numerical parameters chosen, are outlined in this supporting material document. Equations refer to the main document.

References

1. Eberhard Z. 1996 *Oxford users' guide to mathematics* vol. 1. Oxford: Oxford University Press.
2. Hinch EJ. 1991 *Perturbation Methods*. Cambridge University Press.
3. Campbell SL, Meyer CD. 1991 *Generalized inverses of linear transformations*. New York: Dover.
4. Mathworks. 2019 Moore-Penrose pseudoinverse. https://au.mathworks.com/help/matlab/ref/pinv.html. Accessed: 6/3/19.